

Electron impact ionization of N₂ and O₂: contributions from different dissociation channels of multiply ionized molecules

Cechan Tian[†] and C R Vidal

Max-Planck-Institut für Extraterrestrische Physik, PO Box 1603, 85740 Garching, Germany

Received 27 July 1998

Abstract. The cross sections of ionic products due to the electron impact ionization of N₂ and O₂ have been measured for the electron energies from threshold up to 600 eV. The contributions to the cross sections from the possible reaction channels after the multiple ionization of molecules are also determined. The experiment shows that for both N₂ and O₂ the singly charged fragment N⁺ or O⁺ originates mainly (~70%) from the contribution of the dissociation of the singly charged parent ions, whereas the doubly charged fragments N²⁺ or O²⁺ are mainly (~70%) from the dissociation channel of doubly ionized N₂ into N²⁺ + N or O₂ into O²⁺ + O, respectively. At high electron energies, 85% of singly ionized N₂ molecules stabilize into N₂⁺, whereas about 70% of singly ionized O₂ molecules stabilize into O₂⁺. More than 80% of doubly ionized N₂ and O₂ molecules dissociate through the equal charge separation channel. However, after triple ionization, most of the molecules dissociate into two charged fragments. The experiment also shows that the total cross sections for the different ionization stages decrease exponentially as the ionization stage increases.

1. Introduction

The cross sections for electron impact ionization and dissociative ionization of molecules are of fundamental importance in modelling plasmas and understanding the complex ion–molecule reactions in the interstellar environment. However, although experimental work has been done since the 1920's [1, 2], the accurate determination of the total as well as the partial cross sections of electron impact ionization of atoms, molecules, and ions is still an experimental challenge [3]. Especially in the measurement of the partial cross sections for the fragments produced by the dissociation of molecules and molecular ions, which usually carry the kinetic energy of a few electronvolts and can easily escape collection, the reported results show very large discrepancies even for very simple molecules [4–16]. Not until very recently did Straub *et al* realize that it is important to verify the complete collection *experimentally* in order to do conclusive measurements [12–16]. Straub *et al* used a position-sensitive detector and observed the positional distribution of the ionic fragments. They can thus ascertain that all the fragments are collected in the experiments. Alternatively, the present authors developed a focusing time-of-flight (FTOF) mass spectrometer, which has a very high capability of collecting all the fast ions [17, 18]. The complete collection is checked experimentally by observing the deflection curves. The results from the experimental set-ups of Straub *et al* and the present authors, where in both experiments the complete collection is checked experimentally, always agree with each other within experimental error, no matter whether the other previous results agree or not. Hence it becomes possible to obtain *final* cross section data for some molecules. The

[†] Present address: Department of Physics, Texas A&M University, College Station, TX 77843-4242, USA.

higher mass resolution of the FTOF mass spectrometer developed by the present authors also makes it possible to perform measurements for some hydrocarbon molecules [19, 20].

However, if we go one step further, we are confronted with an interesting question. In the electron impact ionization of molecules, the molecules can be either singly, doubly, triply or even more highly ionized. The ion products are formed by the dissociation of the molecules at different ionization stages. How much do the molecules at different ionization stages contribute to the total production of different ionic products? This question has never been answered before for any molecules, although the answer is important in understanding more about the ionization and dissociation of molecules, the electronic structures of multiply ionized molecules and the dissociation dynamics of multiply charged molecules. Recently the structure and the dissociation dynamics of multiply charged molecules have attracted growing interest [21], it thus becomes more interesting to study how much the different dissociation channels of molecules at different ionization stages contribute to the production of the ionic fragments.

In this paper we try to answer this question for the simplest molecules, N_2 and O_2 . In the case of N_2 , since the ion with the highest charge observed in the present experiment is N^{2+} , the different reaction channels after multiple ionization of N_2 can be described by the following reactions:

Single ionization:



Double ionization:



Triple ionization:



From this it is clear where the different fragments come from. Obviously, in the case of O_2 , all the N in equations (1)–(6) should be replaced with O.

In this paper we study the electron impact ionization of N_2 and O_2 with a covariance mapping mass spectroscopic technique [22, 23]. At very low count rates, the covariance mapping mass spectra can be used to interpret the cross section data, where the diagonal elements correspond to the detection of ions, and the off-diagonal elements correspond to the detection of ion-pairs. After appropriate normalization we can obtain the absolute cross sections for the ionic products N_2^+ , N^+ (N_2^{2+}), and N^{2+} (or O_2^+ , O^+ (O_2^{2+}), and O^{2+} in the case of O_2) as well as those for the ion-pair channels (4) and (6). We can thus derive the contributions from the different reaction channels following single, double or triple ionization. The total cross sections for the ionization stages from single, double or triple can also be obtained.

2. Experiment

2.1. Experimental set-up

The experimental set-up consists of a molecular beam crossed with an electron beam, and an FTOF mass spectrometer, which has already been described in detail [17, 18, 24]. Briefly, a CW effusive molecular beam is crossed with a pulsed electron beam (100 ns) at right angles. The

molecular beam is produced by a gas flow from a long needle with a diameter of 0.4 mm passing through a skimmer. The top of the needle is about 2 cm above the skimmer and the skimmer is about 6 cm above the electron beam. The interaction region is less than $4\text{ mm} \times 4\text{ mm} \times 4\text{ mm}$. About 100 ns after the decay of the electron beam a pulsed voltage is applied to the extraction mesh of the mass spectrometer. The ions are extracted into a specially designed FTOF mass spectrometer [17]. The shield plates in the interaction region of the FTOF mass spectrometer make the extraction mesh into a plano-convex lens, which focuses the ions close to the axis of the FTOF mass spectrometer when the ions leave the ion source region. It also reduces the divergence angle with respect to that in the extraction system of a normal Wiley–McLaren TOF mass spectrometer. The flight tube of the FTOF mass spectrometer is segmented into two sections of identical length with a fine mesh in between. The fine mesh performs as a spherically symmetric lens if the voltage applied to it is about 1.3–1.4 times the voltage on the flight tubes. The detection plane is thus the image of the acceleration plane. In the experiments the voltage applied to the extraction mesh is typically -0.85 kV , that on the flight tubes is -1.75 kV , and that on the focusing mesh is -2.33 kV .

As described in detail in a previous publication [17], the focusing effect of the present TOF mass spectrometer raises significantly the tolerance of the detection system with respect to the initial kinetic energy and the starting position of the ions. Ion trajectory calculations show that with the present voltage settings the ions with an initial kinetic energy of as high as $25\text{ eV}/\text{charge}$ can be collected with the same efficiency as the thermal ions in the FTOF mass spectrometer.

The ions are detected with a microchannel plate. The signals are amplified in a fast preamplifier, filtered with a constant fraction discriminator, and counted with a multichannel scalar with a time resolution of 2 ns. The covariance mapping mass spectra are recorded to get both the ion counts and the coincidence counts. The technique of covariance mapping mass spectroscopy was developed by Frasinski *et al* [22, 23]. In this technique the autocorrelation function of each single-shot spectrum is calculated and accumulated. After a long time accumulation the coincidence spectra are illustrated in a two-dimensional map. If the total number of counts in each single shot is very small so that in the single shot the count at each time bin is either zero or one, the accumulated spectrum can be used to determine the cross sections for the ionic fragments as well as the ion-pairs. As described by Frasinski *et al*, the diagonal elements of the covariance mapping mass spectra correspond to the counts for ions, whereas the off-diagonal elements correspond to the counts for ion-pairs. In order to subtract the false coincidence counts, a spectrum accumulated from single-count events is also recorded at the same time, which is used to subtract the false coincidence in a similar way to that of Bruce *et al* [25]. Briefly, the autocorrelation function of the single-count spectrum is calculated, and the amplitude of the islands corresponding to the detection of a pair of a parent and another ion is normalized to that in the accumulated covariance map. Then it is subtracted from the covariance map. After the subtraction we see that only some statistically insignificant fluctuations around zero are left for the islands corresponding to the detection of a parent ion and another ion.

2.2. Normalization to absolute cross sections

The absolute cross sections of the molecules are obtained by normalizing the ion counts to those of a well known gas like argon. Firstly, the ion counts of argon are recorded for electron energies with a particular backing pressure. Secondly, the molecules to be measured are used with the same backing pressure and all other experimental conditions are kept unchanged and the ion counts of these molecules are also recorded. The pressures of the gases in the small

chamber above the needle are kept low enough so that the gas flow is in the effusive flow region. The absolute partial cross sections (e.g. N^+ from N_2) are obtained by

$$\sigma_{N^+} = \frac{I_{N^+}}{I_{Ar^+}} \sigma_{Ar^+}, \quad (7)$$

where I is the number of counts, which is obtained from the diagonal elements of the covariance mapping mass spectra. Argon is used as the reference gas because its ionization cross section has been well established. In this work, the very recent result of Straub *et al* has been taken as the reference value [12]. From equation (7) we can get the partial cross sections for all the ionic fragments. Hence the total cross sections can also be derived.

The absolute cross section of an ion-pair, for instance $N^+ + N^{2+}$, is obtained by

$$\sigma(N^+ + N^{2+}) = \frac{n_{\text{coincidence}}}{n_{\text{total}} T \eta} \sigma(\text{total}), \quad (8)$$

where n_{total} is the total number of ions, $\sigma(\text{total})$ is the total ionization cross section of N_2 , T is the total transmission of the meshes in the TOF mass spectrometer and η is the detection efficiency of the microchannel plate. We get the transmission of the meshes from the measurement of the optical transparency and the open area from the manufacturer's manual. The two data agree with each other. We get $T = 58.1\%$. For the detection efficiency of the microchannel plate, we use the open area ratio from the manufacturer's manual, which is 60%. It has been proven experimentally by a number of authors that the detection efficiency of the microchannel plate is equal to its physically open area ratio [12,26,27]. For getting the data at a particular electron energy, the accumulation takes 2 h at a repetition rate of 5 kHz. Usually the measurements have been repeated at least four times. The statistics are taken to get the final cross section values and the data fluctuations.

2.3. Error estimate

The errors in the cross sections of the fragment ions relative to the total values originate mainly from the data fluctuations, the gas pressure stability in the measurements, and the other isotopes of N or O. The counts from the background gas are measured without the molecular beam and are usually less than 5% of the total counts. They are subtracted. Unless otherwise stated, the error of the partial cross sections with respect to the total cross section is about 6%. The normalization of the data caused an error of 6%. The errors of the absolute cross sections are believed to be about 10%.

A very important error source in the measurement of the cross section of ion-pairs is due to false coincidence. In order to verify how much false coincidence contributes in the present work, we measured the cross sections of ion-pair channels at different count rates by adjusting the molecular density and the electron beam current. The count rates for true coincidence are proportional to the molecular density and the electron beam current, whereas the count rates of false coincidence are proportional to the squares of the molecular density and the squares of the electron beam current. We measured the cross section of ion-pairs at the count rates from 100 s^{-1} to 600 s^{-1} . The results fluctuate within 4% of the amplitude. This suggests that our subtraction of the false coincidence is very effective. The false coincidence thus does not cause a large error in our measurements. Further error sources can be due to the error of the total cross section data of N_2 and O_2 (10%), those of the absolute transmission of the meshes and that of the detection efficiency of the microchannel plate. As a result, we expect that the total error of the measurements for the channel with an ion-pair is about 20%. Because of the dead time ($\sim 4 \text{ ns}$) of the discriminator and the multichannel scaler, the error for the channels with $N^+ + N^+$ and $O^+ + O^+$ is larger. We expect that it is about 25%. We made the compensation

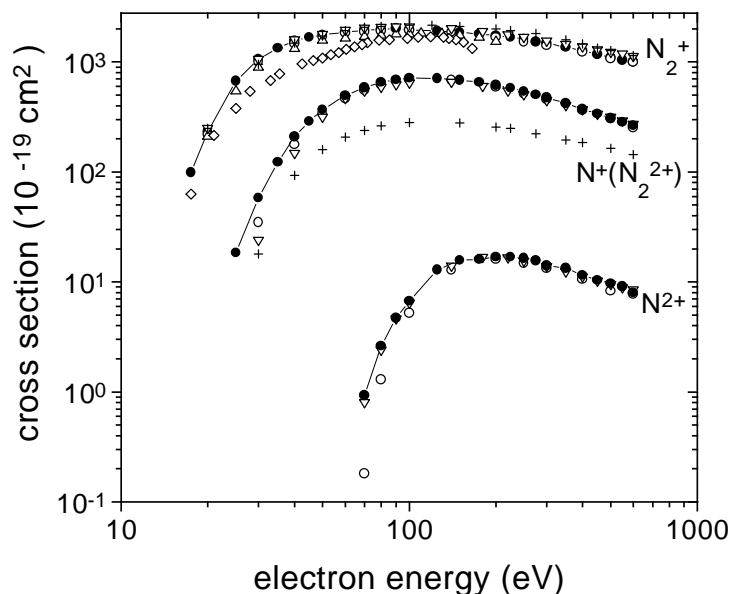


Figure 1. The cross sections for the ionic products from N_2 as a function of electron energy; (—●—) present work.; (○) Straub *et al* [14]; (△) Freund *et al* [28]; (▽) Krishnakumar and Srivastava [29]; (◇) Märk [30]; (+) Halas and Adamczyk [32].

to the dead channels assuming that the peak of the island $N^+ + N^+$ (or $O^+ + O^+$) is flat near the diagonal of the covariance map. For the other channels, the cross section is derived indirectly, the error is expected to be about 25%.

3. Results and discussion

As described above, from the diagonal elements of the two-dimensional covariance mapping mass spectra we get the absolute cross sections for each ionic product. From the off-diagonal elements we get the absolute cross sections for the ion-pair channels, (4) and (6). From the values of the total ionic products and the ion-pair channels, we can deduce all the channels listed in equations (1)–(6) except for channel (3) which is indistinguishable from channel (2) because N_2^{2+} has the same m/e value as N^+ . The results are discussed in the following.

3.1. Results on N_2

The ionic products from the electron impact ionization and dissociative ionization of N_2 include the singly charged parent ion N_2^+ , the doubly charged parent ion N_2^{2+} , the singly charged fragment N^+ and the doubly charged fragment N^{2+} . The cross sections for these ionic products have been measured by Straub *et al* [14], Freund *et al* [28], Krishnakumar and Srivastava [29], Märk [30], Crowe and McConkey [31] and Halas and Adamczyk [32]. The present results, together with the existing data, are shown in figure 1. For N_2^+ we see that the present results agree with all the previous results, except that the data of Märk are lower than the present results and the other data by about 30% at lower electron energies and around 160 eV. For N^+ , where there is some contribution from metastable N_2^{2+} , the present results agree well with the data of Straub *et al* and Krishnakumar and Srivastava. The data of Halas and Adamczyk are

Table 1. The cross sections (10^{-19} cm²) of different dissociation channels after single, double or triple ionization of N₂.

EE	Total production		Single ionization			Double ionization			Triple ionization N ²⁺ + N ⁺
	N ²⁺	N ⁺	N ₂ ⁺	N ⁺ + N	Total	N ⁺ + N ⁺	N ²⁺ + N	Total	
600	8.01	264	1003	168	1172	46.4	4.97	51.4	3.04
550	9.11	282	1037	184	1221	47.9	6.14	54.0	2.96
500	9.68	307	1095	200	1296	51.8	6.64	58.4	3.04
450	10.3	337	1173	217	1391	58.1	7.12	65.3	3.24
400	11.4	372	1270	238	1508	65.0	7.88	72.9	3.60
350	13.3	418	1357	266	1624	73.7	9.07	82.7	4.26
300	14.0	473	1480	298	1779	84.8	9.15	94.0	4.91
275	15.6	504	1531	315	1847	91.8	10.4	102	5.20
250	16.4	540	1623	333	1957	100	10.7	111	5.62
225	16.8	578	1684	358	2042	107	11.0	118	5.82
200	16.8	614	1741	380	2121	114	11.0	125	5.84
175	16.0	657	1797	405	2203	122	10.5	133	5.47
150	15.8	686	1863	424	2288	128	11.3	140	4.44
125	12.8	708	1919	444	2364	130	10.1	140	2.70
100	6.69	712	1961	471	2433	119	5.79	125	0.899
90	4.68	689	2015	472	2487	108	4.10	112.	
80	2.61	655	1977	474	2452	90.1	2.40	92.6	
70	0.927	587	1942	452	2394	67.3	0.883	68.1	
60		495	1865	412	2278	41.2		41.2	
50		367	1772	323	2096	21.7		21.7	
45		288	1676	260	1937	10.0		10.0	
40		209	1564	190	1755				
35		123	1343	110	1454				
30		58.3	1062	52.0	1114				
25		18.4	672	14.0	686				
20			233		234				

lower than the present results by a factor of two.

The present results for the ionic products and different channels after the multiple ionization of N₂ are shown in table 1. After the single ionization, N₂ has two possible channels, which form stable N₂⁺ (equation (1)) or N⁺ + N (equation (2)), respectively. The cross sections for these two channels are shown in figure 2. There might be some contributions from N₂²⁺ to the data of channel (2). From the results on CO we can estimate the contribution since CO and N₂ are isoelectronic molecules. In the electron impact ionization of CO, the cross section of producing metastable CO²⁺ peaks at the electron energy of 120 eV with the value of 8.5×10^{-19} cm² [18]. Hence we expect that the contribution from metastable N₂²⁺ is similar, which is thus negligible compared with the cross section of channel (2). From figure 1 we see that at high electron energies after the single ionization of N₂ 85% of molecules stabilize into N₂⁺. Only a small fraction ($\sim 15\%$) of the N₂⁺ molecules dissociate into an ionic and a neutral fragment.

The cross sections for the equal charge separation channel N⁺ + N⁺ (equation (4)) and the differing charge separation channel N²⁺ + N (equation (5)) after double ionization of N₂ are illustrated in figure 3. The data of the stabilization channel (equation (3)) are missing. However, from the results on CO we estimate that they are comparable with those for the differed charge separation channel. We see that the channel of equal charge separation dominates. The cross section for the differing charge separation is much smaller. In calculating the total cross section

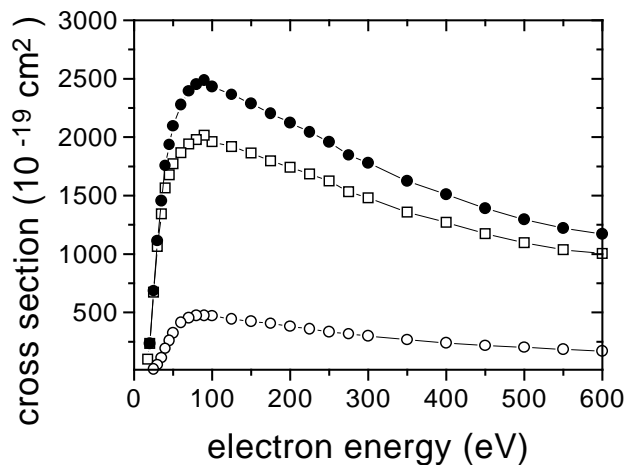


Figure 2. The cross sections of the different channels after the single ionization of N_2 . (\square) stabilization channel N_2^+ ; (\circ) dissociation channel $N^+ + N$ (with negligible contribution of the indistinguishable N_2^{2+}); (\bullet) total cross section.

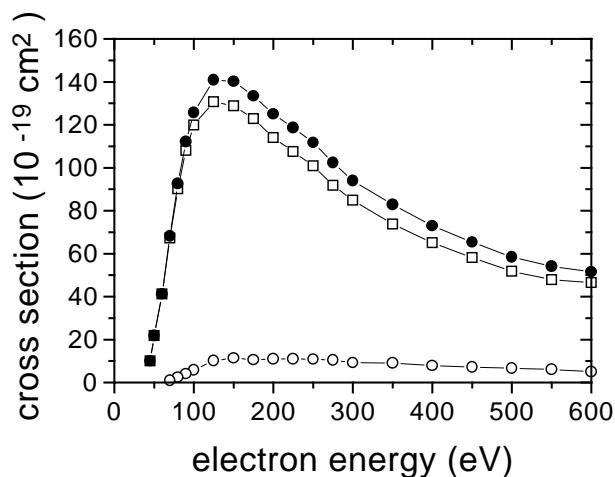


Figure 3. The cross sections of the different channels after the double ionization of N_2 . (\square) equal charge separation channel $N^+ + N^+$; (\circ) differing charge separation channel $N_2^{2+} + N$; (\bullet) total cross section.

of double ionization, we neglected the contribution from the formation of metastable N_2^{2+} , and we expect that this does not cause a big error. At the electron energies near the threshold, there might be contribution from the autoionization of N_2^{+*} to the production of $N^+ + N^+$ [33, 34]. However, we expect that this contribution is much smaller than the contribution from the direct dissociation of doubly ionized N_2 . At high electron energies the total cross section for double ionization is smaller than that for single ionization by a factor of about 20.

Among all the possible reaction channels after the triple ionization of N_2 only the channel of $N^{2+} + N^+$ is within the present experimental sensitivity. The cross section for this channel is shown in figure 4. The cross sections for the other channels are believed to be much smaller, and are thus neglected. Again the total cross section for triple ionization is smaller than that

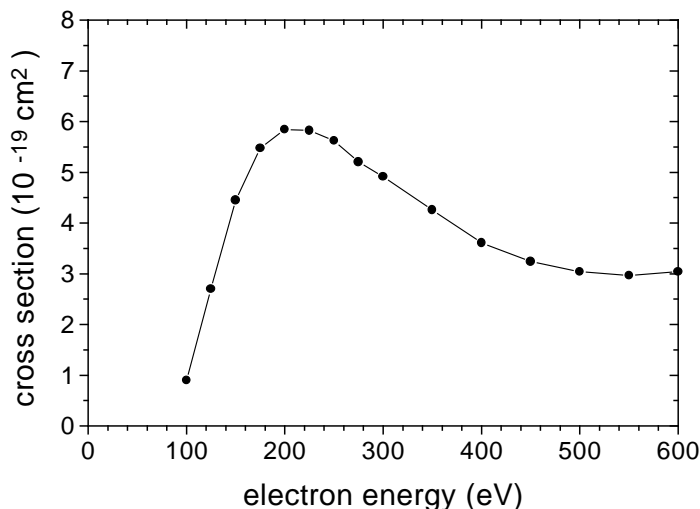


Figure 4. The cross sections of the dissociation channel after the triple ionization of N_2 . (—●—) channel $N^{2+} + N^+$.

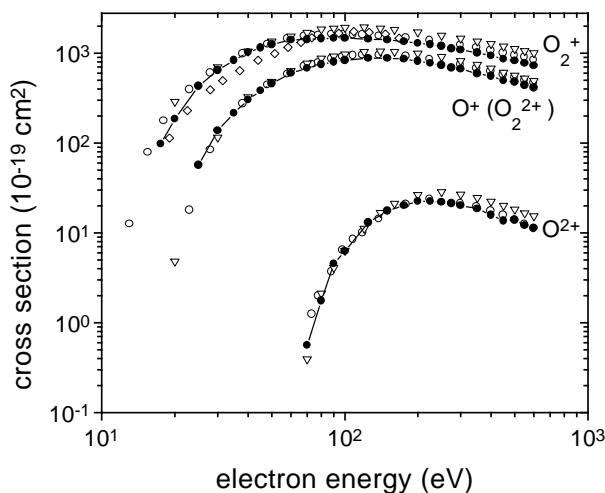


Figure 5. The cross sections for the ionic products from O_2 as a function of electron energy. (—●—) present work; (○) Straub *et al* [14]; (▽) Krishnakumar and Srivastava [35]; (◇) Märk [30].

for double ionization by a factor of about 20.

When we know the cross sections for all the channels after the ionization of N_2 , we can clearly see how much the different channels contribute to the cross sections of the ionic products. For N_2^+ , it is obvious that the contribution is exclusively from the single ionization of N_2 . Whereas for N^+ , at high electron energies, more than 60% of the N^+ production is from the dissociation of singly ionized N_2 . Around 35% of the N^+ ions are produced by the dissociation of doubly ionized N_2 . The contribution from the dissociation of triply ionized N_2 is much smaller. In the production of N^{2+} , at high electron energies, about 60% of the contribution is from the different charge separation channel of the doubly ionized N_2 . The other contribution is from the dissociation of the triply ionized N_2 .

Table 2. The cross sections (10^{-19} cm^2) of different dissociation channels after single, double or triple ionization of O_2 .

EE	Total production		Single ionization			Double ionization			Triple ionization $O^{2+} + O^+$
	O^{2+}	O^+	O_2^+	$O^+ + O$	Total	$O^+ + O^+$	$O^{2+} + O$	Total	
600	11.3	412	726	290	1017	59.2	8.05	67.3	3.29
550	12.0	439	772	314	1087	60.7	8.37	69.1	3.71
500	13.9	477	828	339	1168	66.7	9.82	76.5	4.14
450	13.6	496	864	348	1213	71.8	8.91	80.7	4.77
400	15.8	554	938	387	1326	80.4	10.3	90.7	5.54
350	18.5	593	1010	410	1420	88.5	12.2	100	6.27
300	20.1	668	1091	460	1552	100	12.9	113	7.11
275	21.3	690	1130	470	1600	106	14.0	120	7.33
250	22.0	737	1199	502	1701	113	14.4	128	7.63
225	22.5	775	1255	523	1779	121	14.9	136	7.61
200	22.3	813	1290	549	1839	128	15.2	143	7.12
175	20.2	859	1353	587	1941	132	14.1	147	6.19
150	17.5	875	1399	599	1998	136	12.8	148	4.66
125	13.0	881	1440	620	2060	129	10.6	139	2.48
100	6.25	838	1465	615	2080	110	5.68	116	0.565
90	4.53	800	1466	606	2072	96.6	4.53	101.0	
80	1.76	751	1455	592	2048	79.3	1.76	81.1	
70	0.561	682	1428	559	1987	61.5	0.561	62.1	
60		602	1406	520	1926	40.9		40.9	
50		459	1244	417	1662	20.9		20.9	
45		384	1148	364	1512	10.3		10.3	
40		302	1024	302	1326				
35		216	832	216	1048				
30		137	649	137	786				
25		56.9	431	56.9	488				
20			186		186				
17.5			98.2		98.2				

3.2. Results on O_2

The cross sections for the ionic products due to the electron impact ionization of O_2 are shown in figure 5, together with the results of Straub *et al* [14], Krishnakumar and Srivastava [35], and Märk [30]. All the results agree with each other within the combined experimental uncertainties. We also obtained the cross sections for each reaction channel, which are listed in table 2 and plotted in figures 6–8.

After single ionization, O_2 molecules are more dissociative than N_2 . We find that at high electron energies about 29% of the O_2 molecules dissociate into fragments, where the probability is much higher than that for N_2 . Only about 71% of the O_2 molecules stabilize into O_2^+ . The total cross section for single ionization of O_2 is smaller than that of N_2 by about 14% at high electron energies. However, in the case of double and triple ionization, the total cross sections for O_2 are higher than those for N_2 by about 30% and 10%, respectively. Similarly, in the double ionization, the most abundant channel is due to the equal charge separation. Also in triple ionization, the only identified channel is $O_2^{3+} \longrightarrow O^{2+} + O^+$.

For the total production of the singly charged fragment O^+ , about 70% of the contribution is from the dissociation of singly ionized O_2 molecules. The other part is mainly from the equal charge separation of doubly ionized O_2 molecules. For the doubly charged fragment

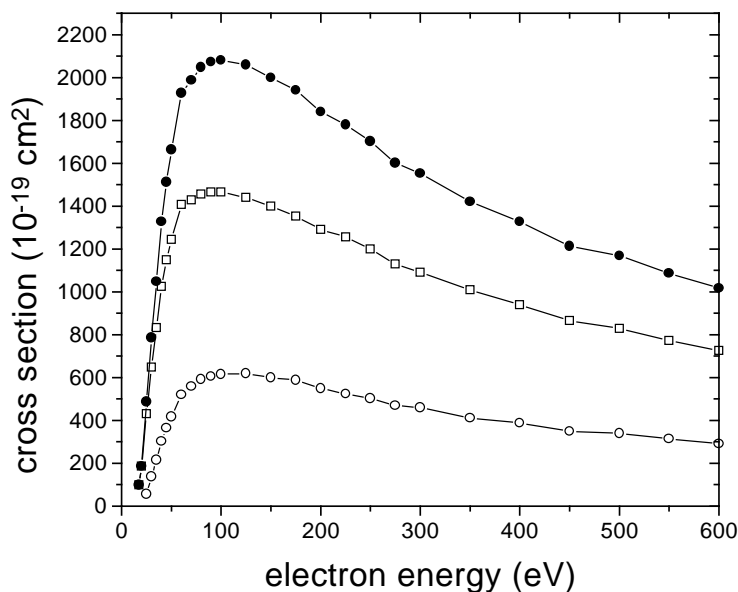


Figure 6. The cross sections of the different channels after the single ionization of O_2 . (—□—) stabilization channel O_2^+ ; (—○—) dissociation channel $O^+ + O$ (with the contribution of the indistinguishable O_2^{2+}). (—●—) total cross section.

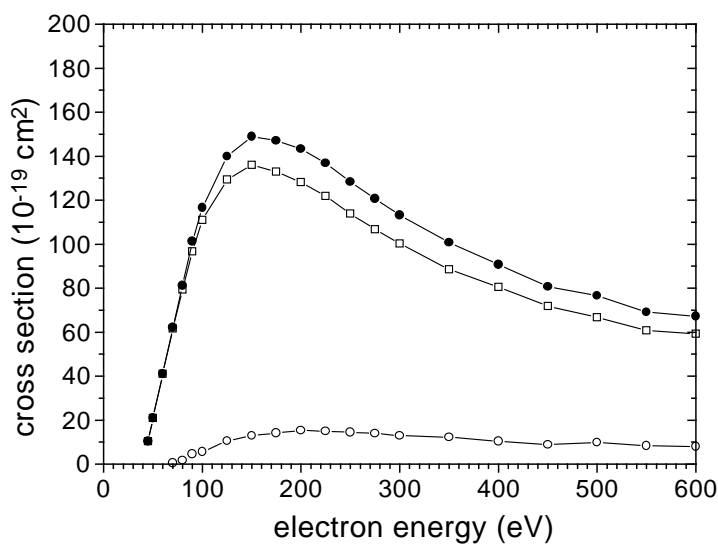


Figure 7. The cross sections of the different channels after the double ionization of O_2 . (—□—) equal charge separation channel $O^+ + O^+$; (—○—) differing charge separation channel $O_2^{2+} + O$; (—●—) total cross section.

O_2^{2+} , 70% of the contribution is from the differing charge separation channel of the doubly ionized O_2 molecules. The triply ionized O_2 molecules contribute to the other fractions.

After we plotted the total cross sections at different ionization stages for N_2 and O_2 versus the ionization stage, we found an interesting feature, which is shown in figure 9. The

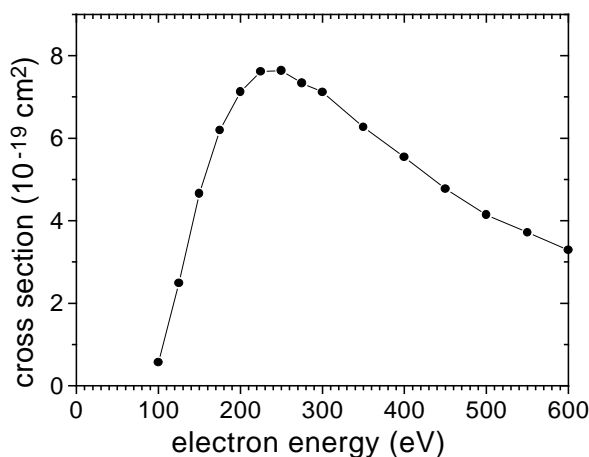


Figure 8. The cross sections of the dissociation channel after the triple ionization of O_2 . (—●—) channel $O^{2+} + O^+$.

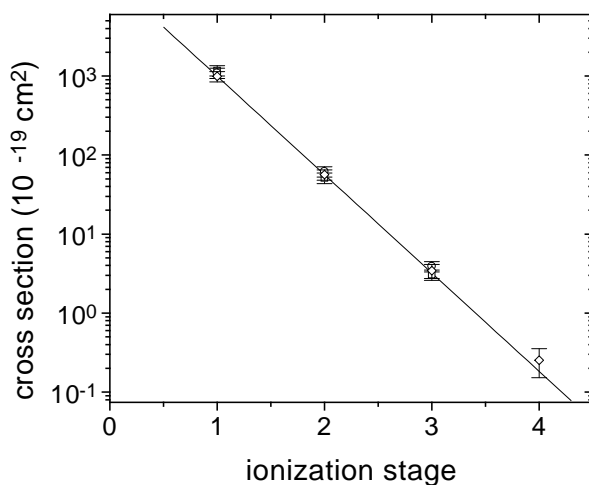


Figure 9. The total cross section of different ionization stages as a function of the ionization stage, the electron energy is 600 eV. (\square) N_2 ; (\circ) O_2 ; (\diamond) CO. Full line: exponential decay.

electron energy is 600 eV. We see that the total cross section shows an exponential decay as the ionization stage increases for both N_2 and O_2 . This indicates that the transition probability from the ground state of N_2 and O_2 to the electronic states of multiply charged molecules decreases exponentially as the charge state increases. This exponential decay was also observed in the multiple ionization of CO [24]. The data are included in figure 9. We also studied this feature at the other electron energies; we found that the total cross sections of single, double and triple ionization show the exponential decay at any electron energies higher than 200 eV, except that the decay rate is slightly different. Since there are no experimental results reported for other molecules, more experimental and theoretical work should be done to understand this feature.

4. Conclusions

The cross sections of ionic fragments and the possible reaction channels after the electron impact multiple ionization of N_2 and O_2 have been measured for electron energies from threshold up to 600 eV. The technique of covariance mapping mass spectroscopy has been used in the measurements. The total production for each ionic product is obtained from the diagonal elements of the covariance mapping mass spectra. The cross sections for the ion-pair productions are obtained from the off-diagonal elements. The experiment shows that, for both N_2 and O_2 , the singly charged fragment N^+ or O^+ is mainly ($\sim 70\%$) from the contribution of the dissociation of singly charged parent ions, whereas the doubly charged fragment N^{2+} or O^{2+} is mainly ($\sim 70\%$) from the differing charge separation channel of the doubly ionized N_2 or O_2 molecules. After single ionization, at high electron energies, 85% of the N_2 molecules stabilize into N_2^+ , whereas about 70% of O_2 molecules stabilize into O_2^+ . After double ionization, more than 80% of the molecules dissociate through the equal charge separation channel. However, after triple ionization, most of the molecules dissociate into two charged fragments. The experiment also shows that the total cross sections for different ionization stages decrease exponentially as the ionization stage increases.

Acknowledgments

CT is grateful to the Alexander von Humboldt Foundation for the financial support for staying at the Max-Planck-Institute for Extraterrestrial Physics. The technical support of B Steffes and the stimulating discussions with T Sykora are also appreciated.

References

- [1] Hughes A L and Klein E 1924 *Phys. Rev.* **23** 450
- [2] Compton K T and Van Voorhis C V 1925 *Phys. Rev.* **26** 436
- [3] Becker K H and Tarnovsky V 1995 *Plasma Sources Sci. Technol.* **4** 307
- [4] Adamczyk B, Boerboom A J H, Schram B L and Kistemaker J 1966 *J. Chem. Phys.* **44** 4640
- [5] Adamczyk B, Boerboom A J H and Lukasiewicz M 1972 *Int. J. Mass Spectrom. Ion Process.* **9** 407
- [6] Märk T D and Hille E 1978 *J. Chem. Phys.* **69** 2492
- [7] Orient O J and Srivastava S K 1987 *J. Phys. B: At. Mol. Phys.* **20** 3923
- [8] Zheng S-H and Srivastava S K 1996 *J. Phys. B: At. Mol. Opt. Phys.* **29** 3235
- [9] Syage J A 1992 *J. Chem. Phys.* **97** 6085
- [10] Wetzel R C, Baiocchi F A, Hayes T D and Freund R C 1987 *Phys. Rev. A* **35** 559
- [11] Tarnovsky V, Levin A, Deutsch H and Becker K 1996 *J. Phys. B: At. Mol. Opt. Phys.* **29** 139
- [12] Straub H C, Renault P, Lindsay B G, Smith K A and Stebbings R F 1995 *Phys. Rev. A* **52** 1115
- [13] Lindsay B G, Straub H C, Smith K A and Stebbings R F 1996 *J. Geophys. Res.* **101** 21 151
- [14] Straub H C, Renault P, Lindsay B G, Smith K A and Stebbings R F 1996 *Phys. Rev. A* **54** 2146
- [15] Straub H C, Lindsay B G, Smith K A and Stebbings R F 1996 *J. Chem. Phys.* **105** 4015
- [16] Straub H C, Lin D, Lindsay B G, Smith K A and Stebbings R F 1997 *J. Chem. Phys.* **106** 4430
- [17] Cechan Tian and Vidal C R 1998 *J. Chem. Phys.* **108** 927
- [18] Cechan Tian and Vidal C R 1998 *J. Phys. B: At. Mol. Opt. Phys.* **31** 895
- [19] Cechan Tian and Vidal C R 1998 *Chem. Phys. Lett.* **288** 499
- [20] Cechan Tian and Vidal C R 1998 *J. Chem. Phys.* **109** 1704
- [21] Larsson M 1993 *Comment. At. Mol. Phys.* **29** 39 and references therein
- [22] Frasinski L J, Codling K and Hatherly P A 1989 *Science* **246** 1029
- [23] Frasinski L J, Hatherly P A, Codling K, Larsson M, Persson A and Wahlström C-G 1994 *J. Phys. B: At. Mol. Opt. Phys.* **27** L109
- [24] Cechan Tian and Vidal C R 1998 *Phys. Rev. A* **58** 3783
- [25] Bruce M R, Mi L, Sporleder C R and Bonham R A 1994 *J. Phys. B: At. Mol. Opt. Phys.* **27** 5773
- [26] Ma C, Bruce M R and Bonham R A 1991 *Phys. Rev. A* **44** 2921

- [27] Brehm B, Grosser J, Ruscheinski T and Zimmer M 1995 *Meas. Sci. Technol.* **6** 953
- [28] Freund R S, Wetzel R C and Shul R J 1990 *Phys. Rev. A* **41** 5861
- [29] Krishnakumar E and Srivastava S K 1990 *J. Phys. B: At. Mol. Opt. Phys.* **23** 1893
- [30] Märk T D 1975 *J. Chem. Phys.* **63** 3731
- [31] Crowe A and McConkey J W 1975 *J. Phys. B: At. Mol. Phys.* **6** 2108
- [32] Halas St and Adamczyk B 1973 *Int. J. Mass Spectrom. Ion Process.* **10** 157
- [33] Lablanquie P *et al* 1989 *Phys. Rev. A* **40** 5673
- [34] Masuoka T and Nakamura E 1993 *Phys. Rev. A* **48** 4379
- [35] Krishnakumar E and Srivastava S K 1992 *Int. J. Mass Spectrom. Ion Process.* **113** 1
- [36] Cechan Tian and Vidal C R 1998 Cross sections for electron impact multiple ionization of CO *Phys. Rev. A* to be published